Instability of Glacial Climate in a Model of the Ocean-Atmosphere-Cryosphere System

Andreas Schmittner,* Masakazu Yoshimori, Andrew J. Weaver

In contrast to the relatively stable climate of the past 10,000 years, during glacial times the North Atlantic region experienced large-amplitude transitions between cold (stadial) and warm (interstadial) states. In this modeling study, we demonstrate that hydrological interactions between the Atlantic thermohaline circulation (THC) and adjacent continental ice sheets can trigger abrupt warming events and also limit the lifetime of the interstadial circulation mode. These interactions have the potential to destabilize the THC, which is already more sensitive for glacial conditions than for the present-day climate, thus providing an explanation for the increased variability of glacial climate.

Early analysis of deep cores from the Greenland ice sheet (*1, 2*) revealed that the North Atlantic climate was much more variable during the last glacial period than during the present interglacial. Meanwhile, numerous observational and model studies implicated that mode changes of the Atlantic THC were involved in these so-called Dansgaard-Oeschger (D-O) oscillations (*3–6*). The reason for the different variability between glacial and interglacial times, however, has remained enigmatic, and the forcing mechanisms for the mode changes are still unknown.

The Atlantic THC currently accounts for up to 1.2×10^{15} W of poleward heat transport (*7*). Near-surface currents bring warm, saline waters from the subtropics to high northern latitudes where they are cooled by the atmosphere, sink to depths between 2000 and 3000 m, and flow back south as a deep western boundary current (*8*).

Since early pioneering studies (*9, 10*), multiple equilibria of the Atlantic THC have been found in a hierarchy of models (*11–13*). Relatively small perturbations to high-latitude surface salinities can lead to the stabilization of the water column, followed by a cessation of deep convection and a subsequent abrupt shutdown of the THC. Sea surface temperatures (SSTs) and sea surface salinities (SSSs) in the North Atlantic consequently drop by several degrees and salinity units, respectively, in agreement with reconstructions of the D-O oscillations (*4, 14*). The reduced northward heat flux also leads to a sudden decrease in near-surface air temperatures in regions adjacent to the North Atlantic (*15, 16*), consistent with proxy records.

Although it seems established that perturbations to the North Atlantic freshwater budget can cause rapid (in less than a century) climate change, little is known about the origins and causes of these freshwater perturbations during the last glacial period, an issue we tackle in the present study. In addition, we address an apparent dilemma concerning the forcing mechanism of the rapid warming events. These events always lag a period of increased iceberg calving (*4, 14*), whereas the input of fresh water associated with the melting of the icebergs is expected to reduce the THC and hence lead to a cooling rather than a warming.

We believe no study to date has incorporated an interactive continental ice sheet model to examine transient THC–ice sheet feedbacks and glacial climate stability, both of which we address as the primary goal of this article. We show that inclusion of active ice sheets causes important differences in glacial climate stability and offers an explanation for the forcing mechanism behind the rapid warming events.

Model, forcing strategy, and coupling strategy. Our Earth System Climate Model (ESCM) uses a fully three-dimensional ocean general circulation model (*17*) coupled to a vertically integrated energy moisture balance model of the atmosphere (*18*). Atmospheric dynamics are absent, and the horizontal transports of energy and moisture are parameterized as diffusive processes. A dynamic-thermodynamic sea ice model (*19*) and a dynamical model of ice sheet flow (*20*) are used as interactive representations of the cryosphere. [For a complete description of each model subcomponent as well as the modern and glacial equilibrium climates, see (*21*).]

The coupling procedure between the ocean-atmosphere–sea ice components and the ice sheet component involves a phase of asynchronous coupling so as to account for the long equilibration time of the land ice component (*22*). During this spin-up phase, the hydrological cycle is not fully coupled (*22*), although upon reaching equilibrium, the ESCM is integrated synchronously for 2000 years with full coupling of the hydrological cycle between the continental ice and the other subcomponent models. The dynamical part of the land ice model is updated once every year using the net annual surface mass balance computed in the atmosphere model. The surface accumulation/melting rate is calculated every atmospheric time step (15 hours) and undergoes the full seasonal cycle. The horizontal model resolution is 1.8° (meridional) and 3.6° (zonal) for all model components. For our simulations of glacial climate we prescribe an atmospheric CO_2 concentration of 200 ppmv and Earth's orbital parameters at 21,000 years before the present (*23*). Present-day wind stress is prescribed for the momentum fluxes at the sea surface for all simulations.

Stability of the Atlantic meridional overturning. The stability of the Atlantic THC is determined by applying a linearly varying perturbation to the surface freshwater fluxes in the North Atlantic (*24, 25*). For present-day conditions, two stable circulation patterns exist (Fig. 1): a state with active North Atlantic deep water (NADW) formation at a rate of around 20 Sv, and a state with no deep water formation. If the system is in a state with active NADW formation, small perturbations lead to linear changes in overturning. A transition to the state without NADW formation ("off" state) can be triggered if a critical threshold is exceeded, and a transition from the "off" to the "on" state occurs when a second threshold is passed. These results are consistent with other model-based studies under modern conditions (*13, 24, 25*).

Qualitatively different equilibria exist under glacial conditions. An interstadial state "I" similar to the modern "on" state is stable for small values of additional evaporation. This state is characterized by strong convection during winter and early spring in large parts of the northern North Atlantic (*26*). Convection depths are largest in the Labrador Sea, just south of Denmark Strait (up to 2000 m), and south of Iceland (up to 1400 m). Surface waters in the southern Norwegian Sea convect to intermediate depths of around 1000 m. If the forcing (the additional evaporation) is turned off, the interstadial state becomes unstable and the system exhibits a rapid change to a state with intermediate overturning strength (~10 Sv). Associated with this transition is a breakdown of convection in the Labrador Sea, in the central parts of the northern North Atlantic, and in the Norwegian Sea. Convection sites shift to the eastern part of the basin to regions west and south of Ireland and to the Bay of Biscay, where surface waters are mixed to intermediate depths of up to 1400 m. These states with intermediate overturning have been found to be stable equilibria in earlier equilibrium simulations of the Last Glacial

School of Earth and Ocean Sciences, University of Victoria, Post Office Box 3055, Victoria, BC V8W 3P6, Canada.

*To whom correspondence should be addressed. E-mail: andreas@ocean.seos.uvic.ca

Maximum with prescribed ice sheets (*27, 28*) and in simulations with an interactive ice sheet in which the hydrological cycle was not fully coupled (*22*). However, in the present model with a fully coupled ice sheet, these intermediate states are only metastable, and they slowly drift (at a rate of ~3 Sv per 1000 years) to the "off" state (*26*), which is characterized by the absence of convective activity in the northern North Atlantic. Sensitivity experiments have shown that this reduced stability of the intermediate states is a consequence of the redistribution of moisture by the ice sheets and shows that the inclusion of fully coupled interactive ice sheets is important even for equilibrium simulations under glacial conditions.

In contrast to the modern case, where only two states are stable, the glacial climate exhibits a metastable (stable for time scales less than a few thousand years) regime of states with overturning strengths of less than 10 Sv, as indicated by the area surrounded by the blue line in Fig. 1A. Transitions between the intermediate states are smooth. However, once the system resides in the stadial regime, extracting freshwater from the North Atlantic can induce a rapid transition to the interstadial state, with the threshold for such a transition being smaller if the initial overturning rate is stronger. Northward advection of saline waters is larger if the THC is stronger and therefore less additional evaporation is needed in order to increase high-latitude salinities to the point where the system switches to the "I" state. The threshold for the "off"-to-"on" transition is very similar for both glacial and interglacial climates. Note that the glacial THC is much more sensitive than the present-day circulation to freshwater perturbations, as indicated by the blue arrows in Fig. 1A.

Feedback between Atlantic overturning and ice sheet mass balance. Before we examine the influence of Atlantic THC mode changes on the mass balance of Northern Hemisphere ice sheets, it is instructive to discuss possible outcomes. Suppose a transition of the THC from a stadial to an interstadial state leads to a massive melting of the continental ice sheets. This could dilute surface waters in the North Atlantic and consequently decrease deep water formation and overturning. In this case, the resulting feedback would be negative. If, on the other hand, ice volume grew in response to a switch to the interstadial state (e.g., as a consequence of an increased atmospheric hydrological cycle), this would extract fresh water from the ocean and lead to a salinification of surface waters. Hence, a further increase in deep water formation would result and the feedback would be positive.

In Fig. 2B we show the model projected change in the ice sheet mass balance directly after a rapid transition to the interstadial state. Because of the warming of near-surface air temperatures by several degrees Celsius (*26*), snowfall increases nearly everywhere over the Northern Hemisphere ice sheets as a consequence of the Clausius-Clapeyron relation. This leads to increased net accumulation over the southern part of Greenland, the eastern part of the Laurentide ice sheet, and the western part of the Scandinavian ice sheet. Around the southern margin of the Laurentide ice sheet and eastern Scandinavia, however, warmer temperatures accelerate melting of the ice in summer, which dominates changes in the surface mass balance there.

A first-order estimate of the sign and magnitude of the feedback can be obtained by integrating the surface freshwater fluxes associated with the ice sheet mass balance over the entire Atlantic drainage basin (*29, 30*). To examine the time evolution of the feedback for a sustained strong overturning, we performed two simulations. After the transition from the stadial to the interstadial "I" state, a constant evaporative forcing is applied to maintain strong deep water formation. The two experiments differ in the value of this sustained forcing. Figure 2C shows the evolution of the feedback for both simulations. During the first 200 years, increased snowfall over the interior ice sheets dominates the changes in the integrated freshwater fluxes in both experiments and the feedback is positive but small (≤0.004 Sv). Larger accumulation over the ice sheets close to the North Atlantic, however, leads to slowly increasing ice thickness and, with a time lag of several hundred years, to increased calving into the ocean. Additionally, the melting of the southern margin of the Laurentide ice sheet and the eastern margin of the Scandinavian ice sheet increases with time. These two processes lead to enhanced freshwater input to the North Atlantic. About 300 years after the switch to the THC "I" state, the feedback becomes negative, as the freshwater flux from the ice sheets into the North Atlantic is now larger than before the mode change. At the margins of the southern Laurentide and eastern Scandinavian ice sheets (blue areas in Fig. 2B), a positive feedback between the ice sheet height and the melting rates leads to accelerated melting. Lowered ice sheet elevations due to surface melting lead to increased summer air temperatures, because of the prescribed atmospheric lapse rate (6.5°C per 1000 m), and hence to further increased melting rates. Mainly as a result of this positive feedback, parts of the ice sheets melt and retreat, and the freshwater flux into the North Atlantic increases with time as the THC remains in the interstadial state. The rapid decreases of the freshwater fluxes after year 1200 are due to vanishing ice at individual grid cells.

The increased freshwater input reaches its largest values of around 0.03 Sv more than 1200 years after the THC mode change. It has the potential to destabilize the interstadial circulation mode, as is most obvious in the experiment with weaker sustained forcing (red lines in Fig. 2C). The variations in overturning during the first 500 years of this experiment are caused by the rapidly changed forcing imposed at the beginning of the experiment. After 500 years, the THC settles in the interstadial state

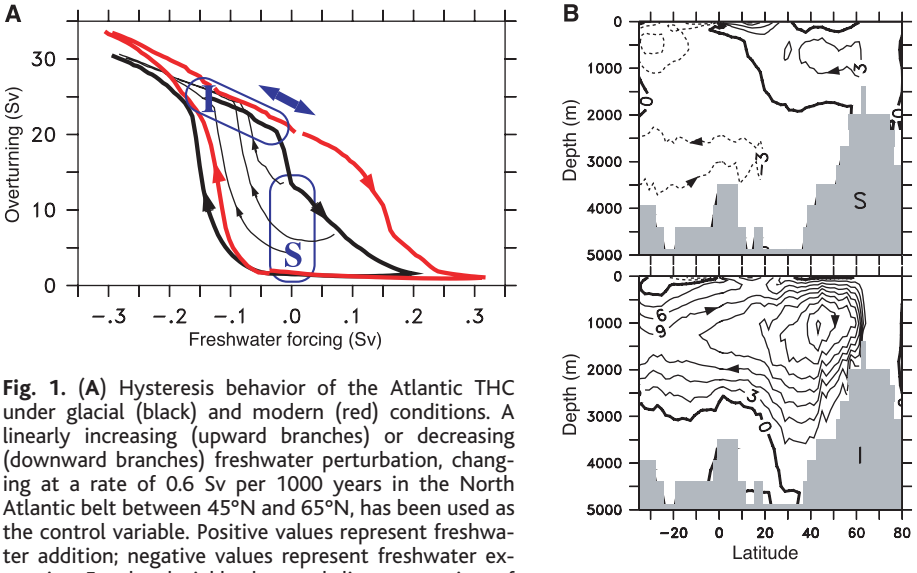

Fig. 1. (**A**) Hysteresis behavior of the Atlantic THC under glacial (black) and modern (red) conditions. A linearly increasing (upward branches) or decreasing (downward branches) freshwater perturbation, changing at a rate of 0.6 Sv per 1000 years in the North Atlantic belt between 45°N and 65°N, has been used as the control variable. Positive values represent freshwater addition; negative values represent freshwater extraction. For the glacial background climate, a regime of metastable stadial states exists with overturning strengths of 10 Sv and less, as indicated by the area including the blue S. Transitions to the interstadial state (blue I) starting from initial conditions with different intermediate overturning strengths are shown as thin black lines. The coupled system is not in equilibrium, as we use a relatively fast rate of change of the forcing. The glacial THC responds with rapid mode transitions for a given perturbation (as indicated by the blue arrows), whereas the response of the modern THC to the same perturbation would be much smaller, linear, and reversible. (**B**) Zonally integrated flow in the Atlantic. Upper panel: a sample metastable, stadial glacial circulation state [indicated by the blue S in (A)]. Lower panel: interstadial state [indicated by the blue I in (A)]. Contour interval is 3 Sv (1 Sv = 10^6 m^3/s).

and this state is stable for more than 900 years, after which the increased freshwater input to the North Atlantic due to the melting of continental ice triggers a rapid transition to a stadial state of intermediate overturning strength. Because of the continued imposed freshwater forcing of −0.05 Sv, the circulation eventually switches back to the interstadial mode. The response of the THC is much weaker for stronger sustained forcing (black lines in Fig. 2C). It decreases only weakly as the freshwater flux into the Atlantic increases as a result of continental ice melting. However, the interstadial state does not collapse. The large imposed evaporative fluxes (−0.08 Sv) lead to a constant increase in North Atlantic salinities, and the freshwater input due to melting of continental ice is considerably smaller (<0.03 Sv) so that it cannot compensate for the imposed forcing.

The fact that we need a sustained prescribed forcing to maintain the interstadial mode in these experiments obscures the response of the THC to the melting of the ice sheets. Nonetheless, from the experiment with the lower value of the sustained forcing, it appears clear that the amplitude of the feedback has the potential to destabilize the warm circulation mode (*31*). In the next section we show that a freshwater forcing of 0.04 Sv can lead to THC mode changes. This is another indication that the amplitude of the feedback we found here (0.03 Sv) is indeed sufficient to trigger mode changes.

How do the relatively coarse resolution [e.g., (*32*)] of the ice sheet model and systematic errors in the simulation of glacial land ice masses affect our results? Comparison of our simulated Laurentide ice sheet with higher resolution models (*33*), with models that include subglacial processes (*34*), and with reconstructions (*35*) suggests that our simulated ice sheet is too high, too steep, and does not extend far enough south. The rate of ice melting (and hence the associated freshwater input to the North Atlantic) in response to the rapid warming depends on the surface area of the ice sheets affected by the rise in the equilibrium line (the altitude below which the net annual mass balance is negative). This area would likely be larger for a more realistic (lower and less steep) ice sheet, which suggests that we probably underestimate the feedback in our model. Therefore, we have reason to believe that the feedback we identify is likely a robust result that would also apply in more realistic, higher resolution ice sheet models.

Reduced calving of icebergs as a trigger for rapid warming. Massive surges of Northern Hemisphere ice sheets punctuated the last glacial period, releasing a great number of icebergs into the North Atlantic, which, as they melted, left traces of their origin (ice-rafted debris, IRD) on the sea floor (*36*). IRD records suggest that after a delay of several hundred years following a major surging event, the climate in the North Atlantic experienced an abrupt change to a warmer state (*14, 37*). It is reasonable to assume, and consistent with IRD records, that after a major surge, the ice streams would have retreated from the coastline, so that the calving rate would have been halted until the ice streams extended back to the shore (*4, 38*). Here we use the ESCM to quantitatively test the effect of reduced iceberg calving on the THC.

Our continental ice sheet model does not exhibit surges, because processes that can lead to surging events such as sliding and the deformation of subglacial sediment in the

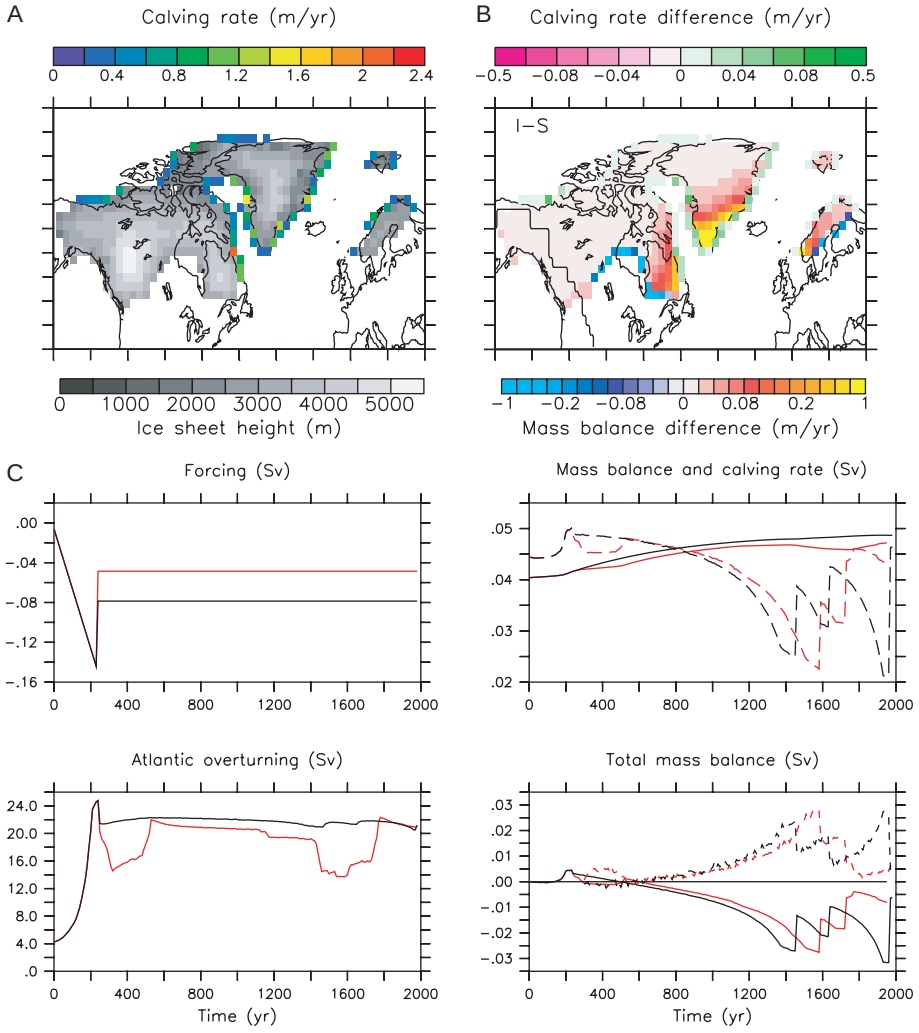

Fig. 2. (**A**) Thickness of simulated major Northern Hemisphere ice sheets (gray scale) and calving rate into the Atlantic (color scale) in the simulation of glacial conditions (state S in Fig. 1). (**B**) Change in surface mass balance (accumulation minus melting; blue-red scale) and calving rate into the Atlantic (purple-green scale) after the system has switched from a stadial (S) state with weak overturning into an interstadial state (I; see Fig. 1). Differences in calving rate between these two states are much smaller than the changes in mass balance (note different scales). The boundary between Pacific and Atlantic drainage basins is indicated by the black line. (**C**) Evolution of the ice sheet mass balance in response to a forced transition of the THC from a weak glacial state to an interstadial state. The forcing is shown in the upper left panel and the THC strength in the lower left panel. Two experiments have been conducted, which differ in the value of the sustained forcing (black line, −0.08 Sv; red line, −0.05 Sv) after the switch to state "I" at year 240. The surface mass balance (dashed line) and calving rate (solid line) integrated over the Atlantic drainage basin are given as equivalent freshwater fluxes in the upper right panel. Their difference, representing the total mass balance changes of the ice sheets in the Atlantic drainage basin, is shown in the lower right panel as anomalies from model year 0 (solid lines). The feedback between the THC and the ice sheet mass balance is positive for positive values of these mass balance changes, and negative for negative values of these changes. Anomalies of the total Atlantic surface freshwater balance (dotted lines) mirror the changes in ice volume. The feedback (solid lines) is initially weakly positive but gets smaller and eventually strongly negative as parts of the ice sheet margin melt and retreat. The associated freshwater flux into the Atlantic has the potential to destabilize the interstadial circulation mode, as is most obvious in the experiment with lower sustained forcing (red line).

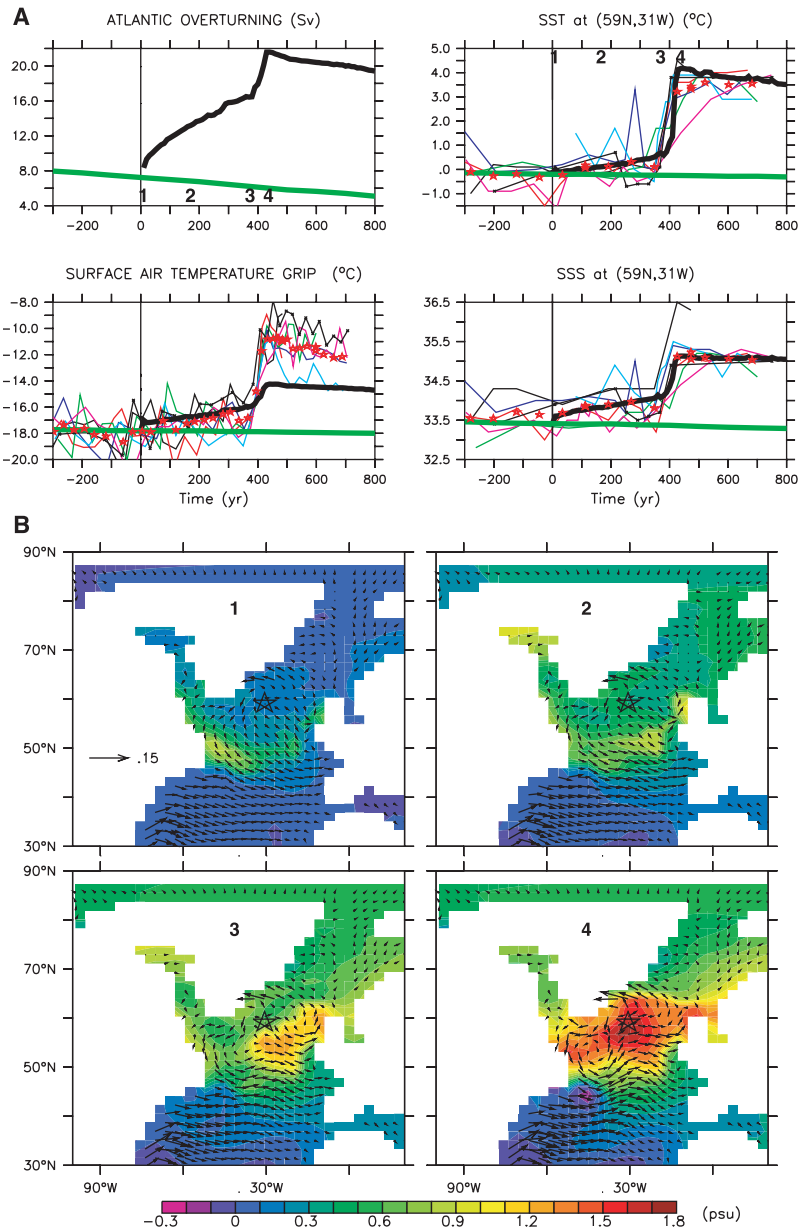

Fig. 3. Response of the ESCM to a cessation of iceberg calving (thick black lines). The control experiment is shown as thick green lines. (**A**) The freshwater flux into the ocean associated with calving of ice sheets (see Fig. 2A) has been set to zero at year 0 (vertical line). Subsequently, overturning in the Atlantic (upper left panel) increases gradually from 7 Sv to about 16 Sv around year 370 (time point 3). A rapid mode change to a present day–like circulation pattern then occurs (time point 4). Surface air temperatures at the location of the GRIP ice core (72.6°N, 37.6°W) increase by about 2°C during this mode change, and SST and SSS in the Irminger Sea (right panels) show an abrupt transition to warmer and more saline conditions. As examples of reconstructed (*14, 39*) rapid warming events at the same locations, D-O events 2 to 8 (~23,500 to 38,500 years before the present) are shown as thin lines of different colors, and their composite is shown as red stars. For the temperature reconstruction over Greenland, a recent estimate for the relation between $\delta^{18}O$ and surface air temperature based on nitrogen and argon isotopes (*40*) has been used. To emphasize the relative changes, we subtracted 4°C (1 psu) from the SST (SSS) reconstruction and shifted the time scale so that the rapid warming occurs roughly at the same time as in the simulation. Simulated SST and SSS changes are in excellent agreement with the reconstruction, both in magnitude and in rapidity, whereas the air temperature response over Greenland is too small (*41*). (**B**) North Atlantic SSS anomaly relative to the start of the experiment (year 0). Annual mean snapshots at time points 1 through 4 [see upper panels in (A)] reveal the initial buildup of SSS anomalies along the northeast coast of North America (point 1), where the freshwater flux anomaly due to the cessation of calving is largest (see Fig. 2A). The SSS anomalies are then transported by the subpolar gyre to the East Atlantic (point 2). They slowly accumulate there (point 3), intensify convection, and eventually result in the rapid transition to the interstadial circulation mode (point 4). Surface currents in m/s are represented by the arrows, and the star at 59°N, 31°W is the location of the time series shown in the right panels of (A).

presence of water are not included. Nevertheless, we can assess the effect of a reduced calving rate on the overturning by setting the freshwater flux associated with ice sheet calving to zero. Results from this experiment (Fig. 3) show that the reduced freshwater input slowly increases surface salinities in the North Atlantic. After a time lag of several hundred years, the climate system switches into a warmer mode. Note that the total freshwater input to the Atlantic ocean due to calving of ice sheets is only 0.04 Sv. From Fig. 1A it seems that this is a relatively small value, and it is surprising that it is sufficient to trigger a THC mode change. However, as we noted earlier, the curves in the stability diagram in Fig. 1A do not represent equilibrium values. Moreover, the spatial distribution of the freshwater fluxes is different between Fig. 1A and the experiment discussed here. Note that the time scale between the surging event and the abrupt warming (~400 years) is in good agreement with the average lead of the IRD maximum with respect to the D-O warmings found in a recent reconstruction from the North Atlantic [figure 7 in (*14*)].

Interpretation and conclusions. We have shown that reduced calving of icebergs into the North Atlantic after a widespread ice sheet surge constitutes a trigger for the rapid glacial warming events. The modeled time scale between the reduced calving and the rapid warming is on the order of a few hundred years, in agreement with reconstructions (*4, 14*). We have also shown that massive melting of lower elevation parts of the ice sheets as a response to a THC transition to the interstadial state can lead to a destabilization of the interstadial circulation mode. This feedback mechanism offers an explanation for the finding from the paleorecord that the climate system during the last glacial period resided in the interstadial state only for a limited period of time. The residence time in the interstadial state varied between a few hundred years and a few thousand years (*1*), and this time scale is consistent with our model results.

Our finding that the stability of the THC in our ESCM is reduced if glacial conditions are applied provides additional reason for the increased variability of glacial climate found in the proxy records. We strongly suggest that interactions between the mass balance of the Northern Hemisphere ice sheets and the Atlantic overturning played a major role in the climate variations around the North Atlantic region during the last glacial period. The time scales associated with these interactions are on the order of several hundred to a few thousand years, which suggests that ice sheet–ocean feedbacks could determine the so far unexplained millennial time scale of the D-O oscillations.

References and Notes

1. W. Dansgaard *et al*., in *Climate Processes and Climate Sensitivity*, J. E. Hansen, T. Takahashi, Eds., vol. 29 of *Geophysical Monograph Series* (American Geophysical Union, Washington, DC, 1984), pp. 288–298.
2. H. Oeschger *et al.*, in *Climate Processes and Climate Sensitivity*, J. E. Hansen, T. Takahashi, Eds., vol. 29 of *Geophysical Monograph Series* (American Geophysical Union, Washington, DC, 1984), pp. 299–306.
3. W. S. Broecker, D. Peteet, D. Rind, *Nature* **315**, 21 (1985).
4. G. Bond *et al*., *Nature* **365**, 143 (1993).
5. T. F. Stocker, *Int. J. Earth Sci.* **88**, 365 (1999).
6. A. Ganopolski, S. Rahmstorf, *Nature* **409**, 153 (2001).
7. M. M. Hall, H. L. Bryden, *Deep-Sea Res.* **29**, 339 (1982).
8. W. J. Schmitz, *Rev. Geophys.* **33**, 151 (1995).
9. H. Stommel, *Tellus* **13**, 224 (1961).
10. F. Bryan, *Nature* **323**, 301 (1986).
11. S. Manabe, R. J. Stouffer, *J. Clim.* **1**, 841 (1988).
12. J. Marotzke, P. Welander, J. Willebrand, *Tellus* **40A**, 162 (1988).
13. T. F. Stocker, D. G. Wright, *Nature* **351**, 729 (1991).
14. S. van Kreveld *et al*., *Paleoceanography* **15**, 425 (2000).
15. S. Manabe, R. J. Stouffer, *Nature* **378**, 165 (1995).
16. A. Schiller, U. Mikolajewicz, R. Voss, *Clim. Dyn.* **13**, 325 (1997).
17. R. Pacanowski, technical report, National Oceanic and Atmospheric Administration Geophysical Fluid Dynamics Laboratory, Princeton, NJ (1995).
18. A. F. Fanning, A. J. Weaver, *J. Geophys. Res.* **110**, 15111 (1996).
19. M. M. Holland, C. M. Bitz, M. Eby, A. J. Weaver, *J. Clim.* **14**, 656 (2001).
20. S. J. Marshall, G. K. C. Clarke, *J. Geophys. Res.* **102**, 20599 (1997).
21. A. J. Weaver *et al.*, *Atmos. Ocean* **39**, 361 (2001).
22. M. Yoshimori, A. J. Weaver, S. J. Marshall, G. K. C. Clarke, *Clim. Dyn.* **17**, 571 (2001).
23. A. L. Berger, *J. Atmos. Sci.* **35**, 2362 (1978).
24. U. Mikolajewicz, E. Maier-Reimer, *J. Geophys. Res.* **99**, 22633 (1994).
25. S. Rahmstorf, *Nature* **378**, 145 (1995).
26. A. Schmittner, M. Yoshimori, A. J. Weaver, data not shown.
27. A. J. Weaver, M. Eby, A. F. Fanning, E. C. Wiebe, *Nature* **394**, 847 (1998).
28. A. Schmittner, K. J. Meissner, M. Eby, A. J. Weaver, *Paleoceanography*, in press.
29. P. U. Clark *et al.*, *Science* **293**, 283 (2001).
30. S. J. Marshall, G. K. C. Clarke, *Quat. Res.* **52**, 300 (1999).
31. The value of the sustained forcing influences the distance to the bifurcation point, and as such it can be regarded as a means to change the stability properties of the circulation.
32. S. J. Marshall, G. K. C. Clarke, *Clim. Dyn.* **15**, 533 (1999).
33. S. J. Marshall, L. Tarasov, G. K. C. Clarke, W. R. Peltier, *Can. J. Earth Sci.* **37**, 769 (2000).
34. J. M. Licciardi, P. U. Clark, J. W. Jenson, D. R. MacAyeal, *Quat. Sci. Rev.* **17**, 427 (1998).
35. W. R. Peltier, *Science* **265**, 195 (1994).
36. H. Heinrich, *Quat. Res.* **29**, 142 (1988).
37. G. C. Bond, R. Lotti, *Science* **267**, 1005 (1995).
38. G. C. Bond *et al.*, in *Mechanisms of Global Climate Change at Millennial Time Scales*, P. U. Clark, R. S. Webb, L. Keigwin, Eds., vol. 112 of *Geophysical Monograph Series* (American Geophysical Union, Washington, DC, 1999), pp. 35–58.
39. S. J. Johnsen *et al.*, *J. Geophys. Res.* **102**, 26397 (1997).
40. N. Caillon, J. Jouzel, J. Chappellaz, *Eos* **82** (fall meeting suppl.), abstract U42A-0011 (2001).
41. The simulated warming of near-surface air temperatures over Greenland (lower left panel in Fig. 3A) is underestimated (2°C) in the model, as compared to about 7° ± 3°C in the reconstructions. The most likely reason for this model discrepancy is related to an underestimation of the northward heat flux into the Nordic Seas and as a consequence to a cold bias over the Nordic Seas in the interstadial state (a known problem in most coarse-resolution models, which also occurs in present-day simulations). Hence, warming of the Nordic Seas due to a restart of the THC is underestimated, and the warming in adjacent regions such as Greenland via atmospheric heat transport is also too small.

42. We thank two anonymous reviewers, O. Saenko, K. Meissner, M. Eby, and S.-Y. Kim for comments. Supported by Natural Sciences and Engineering Research Council of Canada operating grants, Climate System History and Dynamics research grants, the Meteorological Service of Canada/Canadian Institute for Climate Studies (through the Canadian Climate Research Network), and Canadian Foundation for Climate and Atmospheric Sciences.

12 September 2001; accepted 16 January 2002
Published online 31 January 2002;
10.1126/science.1066174
Include this information when citing this paper.

Loss of Sex Discrimination and Male-Male Aggression in Mice Deficient for TRP2

Lisa Stowers,[1] Timothy E. Holy,[2]* Markus Meister,[2] Catherine Dulac,[1]† Georgy Koentges[1]‡

The mouse vomeronasal organ (VNO) is thought to mediate social behaviors and neuroendocrine changes elicited by pheromonal cues. The molecular mechanisms underlying the sensory response to pheromones and the behavioral repertoire induced through the VNO are not fully characterized. Using the tools of mouse genetics and multielectrode recording, we demonstrate that the sensory activation of VNO neurons requires TRP2, a putative ion channel of the transient receptor potential family that is expressed exclusively in these neurons. Moreover, we show that male mice deficient in TRP2 expression fail to display male-male aggression, and they initiate sexual and courtship behaviors toward both males and females. Our study suggests that, in the mouse, sensory activation of the VNO is essential for sex discrimination of conspecifics and thus ensures gender-specific behavior.

Animals have evolved specific communication strategies to identify and attract a mate. Pheromones are a discrete class of chemical cues that signal the sex and the social status of an individual and promote coordinated motor programs and physiological changes essential for breeding and aggression among conspecifics (*1*). The highly reproducible and species-specific character of the response to pheromones offers a valuable experimental system for studying the neural basis of genetically preprogrammed behaviors.

Terrestrial vertebrates have evolved two anatomically distinct sets of olfactory neurons and brain centers to detect and analyze the surrounding chemical world. The main olfactory epithelium (MOE) is located in the posterior recess of the nasal cavity and is accessible to small odorant chemicals carried in the air. The olfactory information detected in the MOE is transmitted to the main olfactory bulb (MOB). Further sensory processing in distinct centers of the primary olfactory cortex and in multiple cortical and neocortical areas generates in humans the distinctive perception of smell (*2*). In contrast, neurons of the vomeronasal organ (VNO) are enclosed within a bilateral and tubular-shaped chemosensory structure of the ventral nasal septum (*3*). In rodents, the VNO opens into the ventral groove of the nasal cavity where it gains access to water-soluble chemical cues carried by the nasal mucus. VNO neurons send fibers to the accessory olfactory bulb (AOB), which in turn projects to discrete loci of the ventromedial hypothalamus via the mediocortical amygdala (*3*). Previous work has suggested that the VNO has a primary role in the detection of pheromones and in eliciting behavioral and physiological responses to conspecifics. Surgical ablation of the VNO in rodents, for example, markedly diminishes mating and intraspecies aggressive behavior of the male and impairs pheromone-induced changes in the estrus cycle of the female (*3*, *4*).

How is the pheromone information detected by chemosensory receptors and transduced into electrical activity by sensory neurons? Molecular studies have shown that MOE and VNO sensory neurons use distinct transduction mechanisms to mediate chemosensory signaling (*5*). In the MOE, specific recognition of odorants is achieved by about 1000 heterotrimeric GTP-

[1]Howard Hughes Medical Institute, Department of Molecular and Cellular Biology, Harvard University, Cambridge, MA 02138, USA. [2]Department of Molecular and Cellular Biology, Harvard University, Cambridge, MA 02138, USA.

*Present address: Department of Anatomy and Neurobiology, Washington University School of Medicine, St. Louis, MO 63110, USA.

†To whom correspondence should be addressed. E-mail: dulac@fas.harvard.edu

‡Present address: Wolfson Institute of Biomedical Research, University College London, London WC1E 6BT, UK.